



Stochastic downscaling of precipitation in complex orography: a simple method to reproduce a realistic fine-scale climatology

Silvia Terzago, Elisa Palazzi, and Jost von Hardenberg

Institute of Atmospheric Sciences and Climate, National Research Council of Italy, Corso Fiume 4, Turin, Italy.

Correspondence to: Silvia Terzago (s.terzago@isac.cnr.it)

Abstract. Stochastic rainfall downscaling methods usually do not take into account orographic effects or local precipitation features at spatial scales finer than those resolved by the large-scale input field. For this reason they may be less reliable in areas with complex topography or with sub-grid surface heterogeneities. Here we test a simple method to introduce realistic fine-scale precipitation patterns into the downscaled fields, with the objective of producing downscaled data more suitable for climatological and hydrological applications as well as for extreme events studies. The proposed method relies on the availability of a reference fine-scale precipitation climatology from which corrective weights for the downscaled fields are derived. We demonstrate the method by applying it to the Rainfall Filtered AutoRegressive Model (RainFARM) stochastic rainfall downscaling algorithm.

The modified RainFARM method has been tested focusing on an area of complex topography encompassing the Swiss Alps, first, in a "perfect model experiment" in which high resolution (4 km) simulations performed with the Weather Research and Forecasting (WRF) regional model are aggregated to a coarser resolution (64 km) and then downscaled back to 4 km and compared with the original data. Second, the modified RainFARM is applied to the E-OBS gridded precipitation data (0.25 degrees spatial resolution) over Switzerland, where high-quality gridded precipitation climatologies and accurate in-situ observations are available for comparison with the downscaled data for the period 1981–2010.

The results of the "perfect model experiment" confirm a clear improvement in the description of the precipitation distribution when the RainFARM stochastic downscaling is applied, either with or without the implemented orographic adjustment. When we separately analyze areas with precipitation climatology higher or lower than the median calculated over all the points in the domain, we find that the Probability Density Function (PDF) of the real precipitation is better reproduced using the modified RainFARM rather than the standard RainFARM method. In fact, the modified method successfully assigns more precipitation to areas where precipitation is on average more abundant according to a reference long-term climatology.

The results of the E-OBS downscaling show that the modified RainFARM introduces improvements in the representation of precipitation amplitudes. While for low-precipitation areas the downscaled and the observed PDFs are in excellent agreement, for high-precipitation areas residual differences persist, mainly related to known E-OBS deficiencies in properly representing the correct range of precipitation values in the Alpine region. The downscaling method discussed is not intended to correct the bias eventually present in the coarse-scale data, so possible biases should be adjusted before applying the downscaling procedure.



Copyright statement. The authors declare that they have no conflict of interest.

1 Introduction

Assessing the impacts of climate change on extreme precipitation events and hydro-meteorological hazards requires reliable precipitation data at fine spatial and temporal resolution. A wide range of downscaling methods has been developed to obtain fine scale precipitation fields from coarse scale data (see Maraun et al., 2010, for a review): Besides physically-based, dynamical downscaling approaches, in which high-resolution regional climate models are nested in global datasets, an effective approach is provided by statistical and stochastic downscaling. While statistical downscaling is based on mapping large-scale predictors for precipitation at small scales (e.g. Maraun et al., 2010; Chiew et al., 2010) to produce the expected small-scale rainfall field, stochastic rainfall downscaling, a type of weather generator, uses information directly from the large-scale precipitation to generate an ensemble of possible stochastic realizations of precipitation fields with a realistic spatial and temporal correlation structure and preserving the large-scale properties of the original field (see e.g. Ferraris et al., 2003).

Stochastic approaches are attractive owing to their computational efficiency, which allows to perform ensemble simulations to evaluate the uncertainties in the small scale precipitation fields, and to their flexibility, as most of them can be applied to a range of temporal scales (Bordoy and Burlando, 2014). Several stochastic downscaling methods have been proposed for precipitation, some of them devised for generating time series at single stations or at a set of stations (Vrac and Naveau, 2007; Mehrotra and Sharma, 2006; Charles et al., 1999; Wilks, 1999, 1998). Here we focus on full-field generators, which have the characteristic of simulating full fields of precipitation, thus providing continuous spatial information usable i.e. as input to distributed hydrological models. Detailed discussions on these models is offered by Bordoy and Burlando (2014) and Ferraris et al. (2003). Full-field weather generators are generally based upon simple autoregressive models, so-called meta-Gaussian models (Rebora et al., 2006), or point process models simulating individual rain cells (Rodriguez-Iturbe et al., 1988, 1987), or spatio-temporal implementation of multifractal cascade models (Lovejoy and Schertzer, 2006; Deidda, 2000, 1999; Lovejoy and Mandelbrot, 1985).

Among the meta-Gaussian models, an example is provided by the Rainfall Filtered Autoregressive Model (RainFARM) procedure, a stochastic rainfall downscaling method based on the extrapolation of the coarse-scale Fourier power spectrum to the small scales. This method was originally developed for spatiotemporal downscaling of rainfall predictions on meteorological timescales (Rebora et al., 2006) and then extended to climatic timescales (D'Onofrio et al., 2014). An advantage of stochastic downscaling methods like RainFARM is that they have few free parameters, they do not require further fields in addition to the original precipitation to downscale and the small-scale correlation structure is estimated from the large-scale field. This makes such methods directly applicable to model outputs also in areas where further fine-scale information is not available. Still, the main limitation of most stochastic downscaling methods is that they do not take into account orographic effects at scales smaller than those resolved by the original precipitation field to downscale. Orographic precipitation mechanisms, such as orographic lifting, play an important role in determining patterns of small-scale precipitation in areas with complex orography (Roe, 2005; Smith, 2006). As a result the fine-scale distribution of precipitation in fields downscaled with e.g. RainFARM



is not conditioned on orography and in particular the long-term climatology at individual grid points may differ significantly from observations. This may make such downscaling method not suitable for applications in which the small-scale hydrological balance is of importance, such as studies involving changes in snow cover or water resources in small mountain basins.

The addition of an orographic component to rainfall downscaling models over land has been investigated, among others, by Harris et al. (1996); Jothityangkoon et al. (2000); Purdy et al. (2001); Pathirana and Herath (2002); Badas et al. (2005, 2006). In particular Harris et al. (1996) and Purdy et al. (2001) were among the first studies using a cascade-based approach to study the multiscale statistical properties of orographic rainfall. Badas et al. (2005, 2006) studied the scaling behaviour of orographic rainfall using a high-temporal resolution rain gauge network in Sardinia, Italy, and developed a modified cascade-based rainfall downscaling model conditioned on local average precipitation and on terrain elevation. These methods require detailed calibration for each study area and the availability of an extensive dataset of local measurements at high temporal frequencies, detailed data which may not be readily available for several regions. Nonetheless, for many areas, information on the spatial distribution of precipitation, at least as a long-term climatological average, may be available from different sources, such as gridded reconstructions based on raingauge observations (e.g. the EURO4M dataset for the Greater Alpine Region, <http://www.euro4m.eu/datasets.html>) or from dynamical downscaling simulations with Regional Climate Models (RCM). In particular non-hydrostatic RCMs, when applied at very fine scales (1 to 5 km resolution), can capture the main physical mechanisms for orographic precipitation and may lead to a realistic spatial distribution of precipitation amounts on average, also over complex topography, albeit often with significant biases in amplitude (Kotlarski et al., 2014; Viterbo et al., 2016).

In this paper we present a very simple approach, described and tested for the specific case of the RainFARM method, which allows to integrate into a stochastic downscaling method information on the fine-scale spatial distribution of precipitation, available from high-resolution gridded observations or from dynamical downscaling. This information is used to modulate locally the distribution of precipitation inside each large-scale grid element of the field to downscale or in the neighbourhood of each point. The precipitation amplitudes on the fine grid are first determined by the stochastic downscaling procedure, then the downscaled precipitation is modulated using the realistic pattern derived from a fine-scale reference precipitation climatology. This last step, consisting in the application of correction factors (or weights), allows to take into account the heterogeneity at the fine scales, including topographic effects. Finally, the overall precipitation amounts at the resolution of the precipitation fields to downscale are adjusted to ensure the conservation of the total precipitation at the large scale, a requirement already present in the standard RainFARM procedure.

We demonstrate the application of the method in two cases. First, in a perfect-model experiment, in which a high-resolution precipitation dataset is first coarse-grained by aggregating it to a coarser resolution and then downscaled with RainFARM, to check for consistency with the original high-resolution field. To this end, a 30-year-long simulation with the Weather Research and Forecasting (WRF) model over Europe (Pieri et al., 2015) is used, providing the reference fine-scale (4 km) precipitation dataset which is first aggregated and then used for validating the downscaled aggregated field. Second, we demonstrate the method in a more realistic setup, by applying it to the E-OBS observational dataset (version 13; Haylock et al., 2008) at about 25 km resolution, and by validating the statistics of the downscaled precipitation fields against surface observations from a dense network of raingauge stations in Switzerland. Since a high-quality precipitation climatology to be used for



calculating correction factors is not always available for many regions of the world, we tested the impact of different reference climatologies on the downscaled fields, considering three different datasets with different degrees of accuracy.

The paper is organized as follows: Section 2 describes the datasets used in this study; Section 3 presents the modifications included in RainFARM to better describe the precipitation at fine scales; Section 4 shows the application and the evaluation of the method, first in a “perfect model experiment” and then in a more realistic case in which E-OBS precipitation is downscaled and the results are compared to surface station measurements; Sections 5 and 6 provide a discussion of the results and the main conclusions of the paper.

2 Datasets

In order to present and validate the method, we employ different precipitation datasets, described briefly in the following:

10 2.1 WRF simulation outputs

In order to perform a “perfect model experiment”, described further on in Section 3.3, we use precipitation data from a very high-resolution climate simulation with the regional climate Weather Research and Forecasting (WRF v3.4.1) model, described in Pieri et al. (2015). WRF was forced in the period 1979–2008 with boundary conditions from the ERA-Interim reanalysis (Dee et al., 2011) and run over the European domain with a double nesting, with a resolution for the inner domain of about 15 0.037° (~ 4 km in the meridional direction). This dataset has been validated through comparison with a range of observation-based and reanalysis datasets (Pieri et al., 2015). In agreement with the general behaviour of several regional (as well as global) climate models which are known to exhibit wet biases over mountainous areas especially in winter (e.g. Kotlarski et al., 2014; Palazzi et al., 2015), also this WRF simulation overestimates precipitation and localized precipitation extremes over the Alps (Pieri et al., 2015).

20 To perform a perfect model experiment we aggregate WRF precipitation data originally available at ~ 4 km resolution to a coarser resolution of 64 km by box-averaging. The coarse-grained field is then downscaled back to 4 km with RainFARM and finally its statistics are compared with those of the original 4 km WRF precipitation. By construction, the results obtained with this approach are not affected by possible biases in the considered datasets, i.e. the total average precipitation mass is the same in the large-scale fields and in the validation dataset.

25 2.2 E-OBS

A more realistic application is provided by a comparison between precipitation downscaled from the European daily observation-based gridded dataset E-OBS (Haylock et al., 2008) and station data. E-OBS provides daily precipitation over land areas from 25°N to 75°N in latitude and 40°W to 75°E in longitude, based on the interpolation of in-situ station data. For the present study we analysed E-OBS precipitation data at 0.25° lat-lon resolution corresponding to about 25 km grid size in the meridional 30 direction. Being based on the interpolation of in-situ stations, E-OBS has potential inaccuracies coming from the interpolation algorithms that are employed and from sampling error related to the capability of estimating reliable grid point values from the



nearest few available stations. This type of uncertainty is largest in areas with sparse and uneven station coverage, in particular in high-elevation regions where the station distribution is biased towards the lower elevations. It also worth stressing that, in general, rain gauges tend to underestimate total precipitation in mountain areas since they do not properly account for snowfall that represents an important contribution in high-elevation regions especially in the cold season.

5 We use the E-OBS gridded dataset as a sample large scale precipitation field to be downscaled with RainFARM. The E-OBS data downscaled at 1 km resolution are then compared with MeteoSwiss station data (described in the following) to check the performances of RainFARM and for validation purposes. It is worth noting that in this, as well as in other, "real case" experiments the conservation mass between the coarse-scale dataset to be downscaled (E-OBS) and the validation dataset (surface stations) is not guaranteed by construction. This source of uncertainty should be considered when evaluating the
10 downscaling performances.

2.3 WorldClim

WorldClim 1.4 (Hijmans et al., 2005) is used here as an example of globally available precipitation climatology which could be used also in regions where no high-quality local gridded data is available. WorldClim consists in a set of global gridded climatologies based on observations with a nominal spatial resolution of about 1 km×1 km. It is a popular choice for ecosystem studies (Bedia et al., 2013; Warren and Seifert, 2011; Peterson and Nakazawa, 2008; Townsend Peterson et al., 2007; Waltari et al., 2007). WorldClim provides 30-year monthly averages of the minimum, mean, and maximum temperature and of precipitation, as well as of other bioclimatic variables, for a reference historical period (1960–1990, labelled as current climate) and for a future period (2050–2080) for four representative concentration pathways (RCPs). Monthly climatologies were obtained from various data sources through spline interpolation methods which use the latitude, longitude and elevation
20 as independent variables. Assessment of uncertainties in the gridded products were made, highlighting that the most uncertain estimates correspond to mountainous and other poorly sampled areas. In fact, Hijmans et al. (2005) compared WorldClim data to two high-resolution datasets in the US and found significant differences particularly in high-elevation regions.

2.4 MeteoSwiss station and gridded data

To validate the RainFARM downscaling algorithm we used the daily precipitation measurements registered by the MeteoSwiss station network. The network comprises about 100 automatic monitoring stations delivering data every ten minutes and about 230 manual stations measuring daily rainfall. MeteoSwiss performs temporal aggregation, gap filling and quality control to correct wrong or implausible measurement values according to agreed protocols (<http://www.meteoswiss.admin.ch/home/measurement-and-forecasting-systems/datenmanagement/data-preparation.html>). Among all the available stations we considered those providing data over the period 1981–2012 and we retained only those with at least 80% of available data, leading to
30 a reduced set of 59 stations, shown in Fig. 1.

We also employed the MeteoSwiss climatology RnormM (Begert et al., 2013) to calculate the corrective weights for the RainFARM downscaling. RnormM provides the monthly precipitation sums over the standard period 1981–2010, calculated from the data of all automatic and manual stations in Switzerland, achieving high accuracy and detailed spatial resolution.



RnormM provides precipitation with nominal spatial resolution of 2.2 km in WGS-84 Long./Lat. coordinates, while the effective resolution, i.e. the average distance between individual weather stations, is 15-20 km. The accuracy of the RnormM analysis depends on the accuracy of the underlying measuring stations and on the ability of the interpolation method employed.

3 The RainFARM stochastic downscaling method and its modification

5 3.1 RainFARM

The RainFARM procedure is described in detail in Rebora et al. (2006) and D’Onofrio et al. (2014), and in the present paper we refer to the spatial-only downscaling method described in the latter. The RainFARM method downscales a large-scale spatio-temporal precipitation field $P(X, Y, t)$, which is considered reliable at scales larger than a reliability scale L_o (which often may coincide with the spatial resolution of the field). Here and in the following we use large-caps coordinates (X, Y) and small-caps coordinates (x, y) to indicate that a field is defined on a coarse or fine grid, respectively.

From the large-scale field to downscale, the method generates a fine-scale field $\tilde{r}(x, y, t)$ at a desired fine-scale resolution by extrapolation of its large-scale power spectrum to the unresolved smaller scales, using the same spectral slope in a log-log plot as the large-scale field, choosing random Fourier phases at small scales and finally using an inverse Fourier transform to return to physical space. Since this procedure by itself would create fields with an unrealistic, almost Gaussian, amplitude distribution, a final nonlinear (exponential) transformation is applied to the resulting field in physical space (von Hardenberg et al., 2003).

In the final step of the procedure, $\tilde{r}(x, y, t)$ is further adjusted to guarantee that when coarse-grained (aggregated) at the large reliability scales, it reproduces exactly the original field to downscale $P(X, Y, t)$:

$$r(x, y, t) = \frac{\tilde{r}(x, y, t) \langle P(x, y, t) \rangle_{L_o}}{\langle \tilde{r}(x, y, t) \rangle_{L_o}}, \quad (1)$$

where the operator $\langle \cdot \rangle_{L_o}$ indicates aggregation (averaging) at scale L_o . This aggregation can consist either in simple averaging over boxes of side L_o , or it could consist in using a smooth operator, such as averaging over a moving circular window with diameter L_o :

$$\langle a(x, y) \rangle_{L_o} = \int_{\Omega} K(x - x', y - y') \cdot a(x', y') dx' dy' \quad (2)$$

where Ω is the entire domain of interest and $K(x - x', y - y') = \theta(L_o^2/4 - (x - x')^2 - (y - y')^2)$ is a kernel representing a circular homogeneous patch of diameter L_o , with θ the Heaviside step function. When the aggregation operator is applied to a large-scale field, the same approach is used, but the field is considered constant over boxes of size L_o , that is the value of a large scale field $A(x, y)$ at a fine-scale point (x, y) is considered to be that at the closest large-scale point $A(X, Y)$, where (X, Y) is the closest large-scale coordinate point. All cases discussed in this work use this smooth approach for the aggregation operator in eq. 1.



3.2 Reproducing fine-scale precipitation climatology in RainFARM

We assume that a reference precipitation climatology $c(x, y)$ at fine spatial scales is available. This could be obtained from long-term time averages of gridded observational datasets of precipitation, radar or satellite observations or from numerical simulations with high-resolution models. This reference climatology is used only to derive local weights used to modify the spatial distribution of precipitation, but the absolute value of precipitation itself is not taken into account, so that possible large-scale biases in the reference climatology are not introduced in the downscaling chain and do not affect the results.

The spatial pattern of precipitation is translated into a map of weights that is used to correct the spatial pattern of the downscaled precipitation fields as follows:

$$w(x, y) = c(x, y) / \langle c(x, y) \rangle_{L_o}, \quad (3)$$

that is, we divide each value of $c(x, y)$ by its local average at scale L_o . Notice that the weights aggregated at scale L_o average to 1. When the spatial average of $c(x, y)$ is 0 (as may happen in arid areas), the weights are all set to 1. If a box-averaging is used for aggregation, the resulting weights field reflects the average climatological distribution in space, inside each cell of size L_o of the climatological precipitation in the reference dataset. In case a smooth moving-window averaging is used for aggregation this is true only in an averaged sense. In general, if the climatology needs to be reproduced at a monthly time-scale, this method can be applied separately for each month, computing separately monthly weights $w_i(x, y)$ from Eq. (3), where $c_i(x, y)$ is the long-term monthly average of the original reference precipitation dataset for month i , with $i = 1, \dots, 12$.

The weights are then applied to the fine-scale fields produced by the RainFARM procedure:

$$\tilde{r}(x, y, t) \rightarrow \tilde{r}(x, y, t) \cdot w(x, y) \quad (4)$$

generating a new field where precipitation is reduced or intensified according to the weights obtained from the long-term climatology. As a last step, the final amplitude adjustment to conserve average precipitation at scale L_o , i.e. Eq. (1), is again applied to $\tilde{r}(x, y, t)$.

The resulting fine-scale field $r(x, y, t)$ still coincides exactly with the large-scale field $P(X, Y, t)$ when both are aggregated at the confidence scale L_o , but its long-term time averaged climatology will reflect on average the small-scale spatial distribution of the reference dataset $c(x, y)$. Notice that the weights in Eq. (3) only use the local distribution of precipitation, but are not sensitive to possible large-scale biases in the precipitation climatology.

4 Results

4.1 Application of RainFARM in a perfect-model experiment

We demonstrate the method using daily precipitation data from long term simulations (1980-2008) performed with the WRF model over the European domain, at 4 km spatial resolution, forced with ERA-Interim reanalysis data (Dee et al., 2011). We focus on the Alpine Region, choosing an area encompassing North-Western Italy and Switzerland (see Fig. 2a). The area comprises 128×128 grid elements of the WRF precipitation fields, $p(x, y, t)$.



The dataset $p(x, y, t)$ is used for the perfect-model experiment, as follows:

- (i) to create the coarse-scale field $P(X, Y, t)$ to be downscaled. $P(X, Y, t) = \langle p(x, y, t) \rangle_{L_o}$ is obtained by aggregating the fine-scale field at scale $L_o = 64$ km, corresponding to 16×16 fine-scale gridpoints, using a box-averaging aggregation;
- (ii) to calculate the reference fine-scale climatology, which is necessary to the modified RainFARM algorithm to estimate the weights;
- (iii) to validate the fine-scale fields produced by the downscaling method. In our example we consider separately monthly climatologies in order to show a general case in which the variability of precipitation at seasonal and subseasonal scales is non-negligible.

The coarse scale field, $P(X, Y, t)$, resulting from the aggregation of $p(x, y, t)$ has 8×8 spatial grid elements. After applying RainFARM to $P(X, Y, t)$, the fine-scale output $r(x, y, t)$ should reproduce as close as possible the climatology and the statistical properties of the original field $p(x, y, t)$.

Figure 2a shows the long-term time-average (1980-2008) of the WRF 4 km resolution precipitation dataset $p(x, y, t)$. The field presents small-scale details which reflect the underlying topography and several topographical features can be easily identified, such as the Apennines mountains in the Italian regions of Liguria and Tuscany (lower corner) or features connected to individual river basins in the Alps. From the small scale field $p(x, y, t)$ we calculate the monthly climatologies, used as a reference to derive the corresponding fine-scale maps of weights, according to Eq. (3).

Figure 2b shows the long-term time-average of the coarse 64 km spatial resolution dataset to be downscaled, $P(X, Y, t)$, obtained by box-averaging aggregation of the fine scale WRF data $p(x, y, t)$. The RainFARM downscaling procedure estimates the large-scale spectral slopes, month by month, directly from the large-scale field $P(X, Y, t)$.

Figure 2c shows the long-term average of the fine-scale fields obtained using the standard RainFARM procedure and using a smooth, moving window with diameter L_o , averaging operator in Eq. (1) for the RainFARM procedure. Since RainFARM alone does not take into account orography at scales smaller than the reliability scale L_o , the climatology of the downscaled field matches the reference climatology only if coarse-grained averages of the downscaled climatology are considered. Inside each grid element of size L_o , the RainFARM field presents a distribution which has no correspondence with the actual reference precipitation climatology. Actually the fine-scale distribution introduced by RainFARM in each large-scale grid element of size L_o is statistically almost homogeneous, as reflected in the smooth distributions found in the long term average (Figure 2c). Indeed if a box-averaging operator had been used in Eq. (1), the resulting climatology of the RainFARM downscaled field would be very similar to Fig. 2b.

Figure 2d is similar to Fig. 2c but shows the results obtained using the *modified* RainFARM algorithm, i.e. applying the weights $w_i(x, y)$ computed from the WRF monthly climatologies. An example of weights map is provided in Fig. 2e which refers to the month of June. In this case the weights correspond to correction factors ranging between 0.4 and 2.4, but similar ranges are found for the other months. Compared to Fig. 2c, in Fig. 2d individual orographic features are now clearly recognizable and there is a significantly improved correspondence with the reference climatology. The improvement gained by the modified RainFARM procedure is better highlighted in Figs. 2f-g which report the anomalies of the climatologies obtained with the different downscaling procedures (Figs. 2c-d) compared to the reference climatology (Fig. 2a). These figures show that



the modified RainFARM algorithm allows to remarkably reduce the bias with respect to the reference climatology both in the valleys and in the mountain ridges. Furthermore, when we compare the climatologies of the standard RainFARM downscaled fields with the reference we find a pattern correlation of 0.81 and a root mean square error (RMSE) of 0.83 mm/day, while the modified method improves these to a correlation of 0.96 and a RMSE of 0.44 mm/day.

5 We proceed investigating to what extent the two RainFARM methods correct the amplitude distributions of the coarse-scale daily precipitation with respect to the reference fine-scale data. Figure 3 shows the PDFs of the WRF daily precipitation before and after application of the downscaling methods. The PDFs are calculated including all the gridpoints of the previously described precipitation datasets, i.e. $8 \times 8 \times N$ gridpoints in the coarse-scale dataset and $128 \times 128 \times N$ gridpoints both in the downscaled and in the validation datasets, N being the number of (daily) time steps in the period 1980-2008. For each down-
10 scaling method (standard and modified RainFARM) we generate an ensemble of 80 stochastic realizations of the downscaled rainfall fields, in order to provide an estimate of the uncertainty associated with the small scale precipitation. In Fig. 3a we report as light-blue and gray shades the spread of the PDF ensembles, as light-blue and gray thick lines the 10th and 90th percentiles of the range of the PDFs obtained with the modified and the standard RainFARM, respectively.

The coarse-scale precipitation fields provide precipitation values mainly below 100-120 mm/day and, in any case, they never
15 exceed 150 mm/day. However, the range of precipitation values simulated at high-resolution (~ 4 km) by WRF extends up to 400 mm/day. The aggregation has clearly smoothed out the precipitation extremes, which appear insufficiently represented in the coarse-scale dataset. Both RainFARM downscaling methods re-introduce high-precipitation values in the range 150-400 mm/day with a probability of occurrence which is comparable to that seen in the original WRF dataset. The PDF of the “real” reference precipitation is included in the range of PDFs obtained via stochastic downscaling: this result confirms the
20 strength of the RainFARM method as a way to effectively represent the upper tails of the precipitation distribution, also when the new modified procedure described in this work is used. In fact, using the modified RainFARM procedure we obtain a similar PDF distribution as in the case of the standard RainFARM, just slightly shifted towards higher precipitation values. The modified procedure, while reproducing better the long-term climatology of precipitation at each point, does not affect the overall capability of the RainFARM method of reproducing extreme precipitation values.

25 In Fig. 3a all gridpoints in the study area have been considered together, mixing pixels with high average precipitation in the climatology and pixels with a lower average precipitation. Since the modified procedure leads to an overall better representation of the downscaled precipitation climatology (Fig. 2d,g), it is interesting to analyse how this is reflected into the representation of the precipitation distribution when gridpoints with low and high precipitation climatology are distinguished. We use the median of the long term climatology (Fig. 2a) as a threshold, in order to separate all pixels into two groups with the same numerosity.
30 Gridpoints with average precipitation climatology above or equal to the median are classified as “high-precipitation” gridpoints, while those with average precipitation below the threshold are labelled as “low-precipitation” gridpoints. For each of the two groups we calculate the PDF of the downscaled daily precipitation and we compare it to the PDF of the original 4 km WRF data in the same group. This exercise is done using both the standard and the modified RainFARM outputs.

Fig. 3b shows the results when the standard (left) and the modified (right) RainFARM methods are applied. When using
35 the standard RainFARM the PDFs of the high and low precipitation gridpoints are separated from each other but for given



precipitation ranges the reference PDF lies outside the range of variability of the PDFs of the downscaled data. Instead, the modified RainFarm is able to capture the reference rainfall PDF, better separating the high from the low precipitation pixels, and the reference PDFs are entirely included in range of PDFs of the downscaled datasets.

In order to better compare the performance of the modified versus the standard RainFARM we show the ratio between the PDFs of the downscaled datasets with respect to the PDF of the reference data: the closer the ratio is to 1, the better is the model performance. The results are reported in Fig. 3c where low and high precipitation gridpoints are shown in the left and right panels, respectively. Also in this case we use the full 80-member ensemble, and the bands in the plot represent the 10 – 90th percentile range. The standard RainFARM shows good skill in representing very rare events with precipitation above 300 mm/day in high-precipitation gridpoints. Apart from this, the standard RainFARM overestimates the frequency of precipitation above few mm/day in low precipitation grid-points and underestimates the frequency of precipitation between few mm/day and 300 mm/day in high-precipitation grid-points. These results show that the standard RainFARM method is, by construction, not sensitive to the differences between low- and high-precipitation grid-points at the fine scale, so precipitation is generally overestimated in low-precipitation gridpoints and underestimated in high precipitation gridpoints (Fig. 3b).

This problem is almost fully corrected when the modified RainFARM is used. The modified RainFARM provides precipitation distributions that are closer to the real one, for almost the full range of precipitation values, for both low- and high-precipitation grid-points. The only exception is for very rare events with daily precipitation above 300 mm/day, occurring in high precipitation gridpoints only, where the standard RainFARM already was showing a good agreement: the frequency of these events is now overestimated with respect to the reference. Apart from this feature the modified RainFARM outperforms the standard method and allows to redistribute in a more realistic way coarse-scale precipitation among the corresponding small-scale gridpoints based only on their average climatology.

4.2 A more realistic test case

In this section we demonstrate an application in which the large scale precipitation field, the reference climatology and the verification data are not derived from the same high-resolution dataset, but from different sources. We downscale the E-OBS dataset, one of the most extensively used gridded observational precipitation datasets over Europe, and we compare downscaled data directly with daily station measurements from MeteoSwiss. The domain of study is again the Swiss Alps, for which a high quality dataset from surface stations is available (Fig. 1). The reference precipitation climatology used to derive the corrective weights is the MeteoSwiss RnormM monthly climatology (see Sec. 2.4), possibly the best available gridded product for the study region. Notice that the MeteoSwiss station data used for verification are included among the stations used to construct this gridded climatology, so it is not independent, but we discuss in a following section the impact of different precipitation climatologies.

We analyze the PDFs of the E-OBS original dataset at 25 km, including only gridpoints/pixels containing at least one surface station. If one pixel includes more than one station the E-OBS time series is repeated in order to have the same number of time series from the surface stations and from E-OBS. As a second step, also in this case, we separate points characterized by “high” and “low” long-term average precipitation. To this end we use the station data and we calculate the long-term average daily



precipitation climatology at each station. The stations are then split into two groups based on the median of the distribution of the precipitation climatologies, so that low-precipitation stations have below-median long-term daily precipitation climatologies and high-precipitation stations have above-median long-term daily precipitation climatologies. The corresponding E-OBS pixels containing the stations are classified based on the classification of the station which they contain.

5 Figure 4a shows the PDFs of E-OBS at its original resolution, of E-OBS downscaled with the standard and the modified RainFARM methods (80 realizations for each experiment) and the PDF of the observations from the 59 stations. The displayed results refer to the case with no distinction between low and high precipitation gridpoints, so all the gridpoints are considered as part of the same sample. In such case the two RainFARM methods provide very similar results, with almost no difference in the 10th and the 90th percentiles of the two PDF distributions. Both downscaling methods introduce variability at small spatial
10 scales, increasing the probability of precipitation events above 100 mm/day with respect to the original coarse scale data. The PDF of the original E-OBS data lies around the lower 10th percentile of the PDF distribution of the downscaled data. The downscaling clearly improves the agreement with observations. Despite this, the probability of occurrence of events above 50 mm/day is still underestimated in the downscaled data with respect to the observations.

To further investigate this result we separate high and low precipitation gridpoints as previously explained and we evaluate:
15 i) the ratio between the PDF of E-OBS data and that of observations, in order to better characterize the E-OBS dataset; and ii) the ratio between the PDF of each downscaling realization (80 realizations for each of the two ensembles) and the observed PDF, in order to characterize the performances of the two downscaling methods (Fig. 4b). The closer the PDF ratio to 1, the better the agreement with the observations. Please note that the shown precipitation range corresponds to the full *observed* precipitation range by construction.

20 When considering low precipitation gridpoints, E-OBS at the original spatial resolution shows a clear tendency to overestimate the frequency of precipitation events from few mm/day up to about 80 mm/day. Above this precipitation threshold the events become rare and the probability of occurrence goes to 0 above 150 mm/day. The small-scale fields obtained with the standard RainFARM downscaling method inherit the overestimation errors in the range between few mm/day and about 80 mm/day. The standard method acts mainly on the tails of the distribution by amplifying the frequency of heavy precipi-
25 tation events. Their frequency becomes comparable or even higher with respect to observations between about 120 and 150 mm/day. If the modified RainFARM algorithm is applied, the PDF ratios get close to 1 throughout the range, showing a clear improvement in the representation of the precipitation distribution with respect to the standard RainFARM method.

When considering high precipitation gridpoints, E-OBS at the original spatial resolution shows important deficiencies and limited capability to reproduce the observed PDF. The agreement between the E-OBS PDF and the observed PDF drops
30 after about 20 mm/day and gets close to zero in the range between 100-300 mm/day. Such inadequacy found for the E-OBS dataset is expected to be reflected to some extent also in the downscaled data. In fact, we find that, with respect to E-OBS at its original spatial resolution, both downscaling methods correctly increase the frequency of high precipitation events and they contribute to reduce the discrepancy with respect to the reference dataset, with the modified RainFARM outperforming the standard RainFARM method. In short, both downscaling methods improve the description of the tail of the precipitation



distribution but the discrepancy between the original coarse scale dataset and the observations is too large to be cancelled out by the downscaling method only.

To further investigate and better characterize the criticalities emerged in high-precipitation gridpoints, we compare the E-OBS PDF and the reference PDF separating the precipitation data according to the seasons (Fig. 4c, left). The agreement
5 between E-OBS and the stations is close to 0 for precipitation events above 100 mm/day in all seasons except winter. It is unlikely that E-OBS coarse-scale precipitation is more reliable in winter months than in the other seasons (see e.g. Turco et al., 2013), rather this result can be explained by worse performances of the station measurements in winter, as in the cold season stations fail to catch most of the solid precipitation and they are prone to underestimation of the total precipitation, especially at high elevations (Rasmussen et al., 2012). Disregarding the likely discrepancy of E-OBS and observations with
10 respect to the *real* winter precipitation amounts, this example is however illustrative because it shows that, if the range of daily precipitation amounts in the coarse-scale dataset overall matches the observed daily precipitation range, as it occurs in winter, the downscaling methods are effective at amplifying the probability of occurrence of the upper tails of the distribution and they successfully reconstruct a PDF similar to the observed one (Fig. 4c, right). Also in this case the modified RainFARM algorithm outperforms the standard version and allows for a closer reproduction of the reference PDF.

15 4.3 Sensitivity of the method to the reference precipitation climatology

The results described in the previous section have been obtained employing a high-quality reference precipitation climatology for the calculation of the corrective weights. The availability of such a high quality dataset is quite rare in mountain regions, allowed here by the fact that the Alps are among the most instrumented mountain regions of the world. Such an amount of high-quality data could be unavailable for other regions in the world. For this reason we explore the sensitivity of the
20 modified RainFARM algorithm to the accuracy of the reference precipitation climatologies and we show possible alternatives if a high-quality gridded precipitation climatology is not available. In these cases, one possibility is to use, for example, a high-resolution global precipitation gridded climatology such as WorldClim, already described in Sec. 2.3, which provides monthly climatologies at 1 km resolution based on more than 47000 stations distributed around the globe. Clearly, the distribution of the stations is uneven and reflects the level of economic development and the population density of a country, as well as the
25 national data access policies, so the uncertainty in areas with low station density can be remarkable (Hijmans et al., 2005). Even in station-dense area such as the Swiss Alps the station database used for WorldClim v1.4 counts only 22 stations (Hijmans et al., 2010), so much less dense than that used to compile the regional-scale MeteoSwiss RnormM climatology (Begert et al., 2013), and consequently likely characterized by lower accuracy.

Figure 5 compares the results of the downscaling performed using weights derived by three different climatologies, i.e.
30 MeteoSwiss, WorldClim and WRF 4 km resolution climate simulations. Owing to the heavy computational costs, we use an ensemble of 10 realizations (instead of 80 as previously done for Figs. 3 and 4) for each of the three experiments. The use of a smaller ensemble does not affect the results, as is evident from the comparison of the two experiments performed with MeteoSwiss weights in Fig. 4b (80 realizations) and in Fig. 5 (10 realizations), respectively. Moreover, keeping in mind the issues of E-OBS (see Section 4.2) regarding its limited capability of describing the observed precipitation range for high



precipitation gridpoints and the consequent difficulties in disentangling the E-OBS limitations from the downscaling method limitations, here we focus the analysis on the low-precipitation gridpoints which are not affected by these problems.

When the WorldClim climatology is used as a reference in the RainFARM downscaling processes, the downscaled output is very close, almost indistinguishable, from that obtained with the more accurate MeteoSwiss climatology (Fig. 5). So, the
5 WorldClim dataset is found to be suitable to be used in the RainFARM stochastic downscaling procedure in this area, suggesting that it may be useful also in other areas of the world when no better alternative is available.

Apart from WorldClim, a second possible option in absence of a trusted, high-resolution gridded precipitation climatology over the domain of interest could be to use a reference climatology derived from very high resolution regional climate model simulations. To address this possibility we test the use of the same WRF climatology at 4 km resolution already exploited in
10 the “perfect case experiment”, this time applied only to derive the weights for the correction in Eq. (4). The use of the WRF climatology provides worse performances compared to the previous experiment with WorldClim (Fig. 5), in particular it leads to an underestimation of the frequency of precipitation amounts between few mm and 120 mm/day. A positive remark is that the values above about 120 mm/day, i.e. the tails of the distribution, are reproduced with the correct frequency. The limitations of the WRF weights approach might be due to the lower spatial resolution of the WRF precipitation dataset (4 km) with respect to
15 MeteoSwiss and WorldClim dataset (~ 2 and ~ 1 km respectively), in turn reflected in smooth weighting factors, biased toward lower values with respect to the corresponding finer resolution MeteoSwiss weights. In conclusion, in our experiment the use of a slightly coarser-resolution (4 km) precipitation climatology results in lower skills in capturing the correct distribution of precipitation amplitude with respect to using the WorldClim fine-scale (1 km) global climatology.

5 Discussion

20 A simple modification to take into account precipitation variability at scales of the order of 1 km into stochastic precipitation downscaling methods has been proposed, applied to RainFARM and tested in the Swiss Alps in two different cases. First, in the so called “perfect model” framework, high-resolution WRF simulations (0.037° , ~ 4 km) have been upscaled to 64 km resolution in such a way that the amount of precipitation in a gridpoint at coarse-scale is, in average, the same as the precipitation fallen in the corresponding 16×16 gridpoints in the original fine-scale field. The downscaling procedure applied
25 to this coarse-scale dataset shows a very good agreement with the “true” precipitation data in terms of its amplitude distribution. When analyzing separately gridpoints with low and high-precipitation climatology (low and high with respect to the median of the daily average precipitation climatologies over the domain), the added value of new RainFARM version over the standard RainFARM is evident. The new version allows to reproduce with very high accuracy the distribution of precipitation in low and high-precipitation gridpoints respectively, remarkably better than the standard RainFARM.

30 Second, we considered a more realistic application in which E-OBS gridded precipitation data are downscaled over Switzerland at about 1 km spatial resolution and then compared to in-situ observations from the MeteoSwiss network. In this case a preliminary evaluation of the E-OBS dataset revealed important discrepancies compared to the observations in high precipitation gridpoints. In fact, in high-precipitation gridpoints the frequency of precipitation events from few mm/day up to 100



mm/day is severely underestimated, particularly for higher precipitation, and events with precipitation above about 100 mm/day are simply not represented in autumn, spring and summer. In these seasons both downscaling methods allow to reproduce larger precipitation values, so that downscaled precipitation values cover the full observed precipitation range, but the frequency of intense events is still severely underestimated with respect to observations. In the winter season, although the frequency of intense events is generally underestimated, the ranges of precipitation values covered by E-OBS are similar to the observed ones. In this case the modified RainFARM method is successful in almost fully correcting the downscaled precipitation fields for the most intense events. In all cases the modified RainFARM outperforms the standard RainFARM method by leading to a better agreement of the distributions compared to observations.

The better agreement between E-OBS and surface stations during the winter season for high precipitation gridpoints is likely due to a balance between different errors: the well known E-OBS underestimation documented for example in Turco et al. (2013) is likely lightened by the undercatch of solid precipitation in surface stations. Even though in E-OBS the frequency of intense precipitation events is still underestimated, at least the ranges of precipitation values are similar in both datasets, and such cases are found to be properly handled by the proposed downscaling method.

The two experiments discussed in this paper, in a "perfect model" and a "realistic case" framework respectively, provide complementary results regarding the skills of the presented downscaling method, and they clearly show what we can expect (or not) when it is used in practical applications. In the "perfect model" experiment there is exact conservation of the water mass between the coarse-scale dataset to downscale and the validation dataset, as the former has been derived by aggregation of the latter. This implies that the error associated with the validation dataset is zero and the degree of agreement between the downscaled and the validation data is an exact measure of the skills of the downscaling method. This experiment shows the very good performance of the modified RainFARM in adjusting the PDF of the downscaled data in such a way that they are not distinguishable from the reference PDF. On the other hand, in the "real case" experiment, the mass conservation between the coarse-scale and validation datasets is not to be expected owing to their very different nature and characteristics. In fact, E-OBS is a 25 km resolution dataset generated interpolating measurements from a small ensemble of surface stations in Switzerland, precisely 13 stations located at elevation not higher than 600 m a.s.l (source E-OBS documentation, <http://www.ecad.eu/>) while elevations between 600 and 4600 m are completely neglected. On the contrary, the validation dataset consists of 59 stations representative of elevations up to 3302 m a.s.l., 50% of these stations lying *above* 600 m, in detail: 25% in the range 600-1600 m, 10% in the range 1600-2000, 10% above 2000 m and 5% above 2500 m. Clearly, the reduced number of underlying stations in E-OBS, together with the station biased toward low elevations, contribute to large uncertainties and discrepancies with respect to the station data, especially in areas prone to high precipitation (Figure 4c).

Among the other sources of errors affecting the downscaled fields in the "real case experiments", the fine-scale climatology used to derive the correction factors (weights) has to be considered. In our case the MeteoSwiss RnormM climatology is probably affected by similar sources of uncertainty as the E-OBS dataset, but to a smaller extent owing to the higher density of stations included and their better altitude representativeness. In detail, RnormM is also derived by interpolation of data from surface stations whose average distance is 15-20 km. The interpolation tends to smooth out peaks and troughs in a surface, so we can expect that the interpolation product provides lower precipitation extremes than the original point measurements. As a



consequence, the resulting RnormM climatology, as well as the maps of weights, are smoothed out with respect to the single surface station climatology, with evident impacts on the agreement between downscaled fields and validation (surface station) reference.

Despite the real case experiments are generally characterized by errors and/or biases both in the coarse-scale datasets to
5 downscale, in the climatology used to derive the weights and in the validation datasets, we have shown that when the range of precipitation variability is at least roughly represented in the large scale dataset, the RainFARM downscaling method is effective in at worst improving, but in most cases correcting, the amplitude distribution of precipitation.

The modified RainFARM algorithm has been shown to provide robust results also in absence of a regional, accurate, fine-scale precipitation climatology tailored on the area of study. In fact, a fine-scale global monthly precipitation product such
10 as WorldClim (at 1 km spatial resolution, but obtained from a limited number of measurement stations) has been shown to provide sufficient information for the weights calculation so that the outputs of the downscaling are indistinguishable from those derived in the "optimal case" using the regional and more accurate MeteoSwiss climatology. This suggests that the modified RainFARM method could be applied also in regions of the globe where only limited climatological information is available, such as that provided by the WorldClim dataset. Since RainFARM does not require to provide or tune additional
15 parameters it could then be applied directly to the coarse-scale dataset to be downscaled.

In the simple method which we presented, downscaled precipitation data in each pixel and for each month are corrected by a constant factor each time precipitation occurs. This is of course an approximation which only modifies the amplitude of precipitation events in that point and not their frequency. The same climatological average precipitation at a point could be obtained either modifying the event frequencies or their intensities. Nonetheless we have seen that the RainFarm method
20 allows to reconstruct plausible fine-scale precipitation values with a frequency of occurrence in agreement with observations, when statistics over 30 years are considered. This makes the new RainFARM approach suitable for downscaling climate model data, when we need to describe the statistics of precipitation characteristic over long (climatic) time scales, and we are not interested in temporal correlations with the observed fields at finer temporal scales. Further work should be done to assess if the new RainFARM algorithm provides added value when the temporal correlation between the downscaled data and the
25 observation is of importance.

The proposed method has been developed and tested in a mountain environment but it could be used, in principle, also in other areas of the globe. In such extended framework, the more general added-value brought by the new RainFARM algorithm is the reproduction of an observed precipitation pattern, no matter if it originates from topography or other surface heterogeneities. When the reference precipitation fine-scale climatology is almost constant over a portion of the domain, or zero as
30 for example in very arid or desert areas in summer months, the resulting weights are all one and the modified RainFARM method provides results identical to those of the standard RainFARM method.



6 Conclusions

Stochastic precipitation downscaling methods generally do not take into account local precipitation patterns at spatial scales below those explicitly resolved in the coarse scale dataset. We propose a simple technique that can be applied to stochastic precipitation downscaling methods to improve the representation of the fine-scale daily precipitation in complex and spatially heterogeneous regions, such as mountain areas. The application of this method requires exclusively fine-scale information on the monthly precipitation climatology from an external reference dataset.

This technique, here applied to the RainFARM stochastic downscaling algorithm, adjusts the fine-scale daily precipitation values calculated by the standard RainFARM method by using monthly sub-grid weights derived by the monthly fine-scale climatology and, lastly, it imposes the conservation of the water mass from the coarse-scale dataset to the downscaled dataset. In our perfect-model experiment, compared to the standard RainFARM the modified RainFARM allowed to reduce the root mean square error on the long-term precipitation climatology from 0.83 mm/day to 0.44 mm/day, thus introducing clear improvements in the downscaling performance. The modified RainFARM has been shown to assign precipitation values to the small scale grid in such a way that when pixels with low or high average climatological precipitation are considered separately, the distributions (PDFs) of the downscaled precipitation are closer to the PDFs of the corresponding reference/observed values. Given its ability to reconstruct the overall precipitation distribution, the modified RainFARM downscaling method can be employed in a number of applications, including the analysis of extreme events and their statistics, and hydro-meteorological hazards.

Like the standard RainFARM, the new RainFARM downscaling method is not intended to correct the biases affecting the coarse-scale dataset. Prior to applying the downscaling, it is recommended to evaluate the degree of agreement between the coarse-scale and possible verification datasets. If the coarse-scale datasets presents clear deficiencies or its long-term climatology is substantially different from the observed/reference climatology so that the conservation of the water mass is strongly violated, bias-adjustment of the coarse scale dataset prior to applying the downscaling could be applied.

The proposed method can be useful in particular for downscaling climate model data, and for any application for which a correlation over fine temporal scales between the downscaled and the observed data is not required. Further work should aim to investigate if this method employing fixed monthly correction factors improves the downscaling performance also when the spatial structures of precipitation have to be reproduced at fine (daily or sub-daily) temporal scales such as applications of downscaling at weather time scales.

In absence of a high-quality fine-scale precipitation climatology at regional scales, also global datasets such as WorldClim could be successfully employed and they provided good performance in our study area.

In conclusion, in spite of its simplicity, the proposed method is found to introduce realistic small scale variability in coarse-scale precipitation fields using only a fine scale monthly precipitation climatology, and it could be applied in different regions of the world, not only mountain areas, to provide a more realistic representation of the distribution and the climatology of precipitation.



Code and data availability. RainFARM has been conceived as an open source command line software, freely available at the link <https://github.com/jhardenberg/RainFARM.jl> All the data sets used in this study are publicly accessible and were downloaded from the following websites: WRF: <http://nextdatapoint.hpc.cineca.it/thredds/catalog/NextData/eurocdx/h1e4/catalog.html>; EOBS: <http://www.ecad.eu>; RnormM monthly precipitation climatology: <http://www.meteoswiss.admin.ch/home/climate/past/climate-normals.html>; MeteoSwiss daily precipitation from surface station, accessible upon registration: <https://gate.meteoswiss.ch/idaweb/login.do>; WorldClim monthly precipitation climatology: <http://www.worldclim.org>.

Competing interests. The authors declare that they have no conflict of interest.

Acknowledgements. This work has received funding from the European Union's Horizon 2020 research and innovation programme under Grant Agreements No. 641762 (ECOPOTENTIAL) and by the Italian project of Interest NextData of the Italian Ministry for Education, University and Research. We acknowledge the contribution of the C3S 34a Lot 2 Copernicus Climate Change Service project (C3S-MAGIC), funded by the European Union, to the development of software tools used in this work. Part of this work has been performed in the framework of the MEDSCOPE (MEDiterranean Services Chain based On climate PrEdictions) ERA4CS project (Grant Agreement N° 690462) funded by the European Union.



References

- Badas, M. G., Deidda, R., and Piga, E.: Orographic influences in rainfall downscaling, *Adv. Geosci.*, 2, 285–292, 2005.
- Badas, M. G., Deidda, R., and Piga, E.: Modulation of homogeneous space-time rainfall cascades to account for orographic influences, *Nat. Hazards Earth Syst. Sci.*, 6, 427–437, 2006.
- 5 Bedia, J., Herrera, S., and Gutiérrez, J. M.: Dangers of using global bioclimatic datasets for ecological niche modeling. Limitations for future climate projections, *Global and Planetary Change*, 107, 1–12, 2013.
- Begert, M., Frei, C., and Abbt, M.: Einführung der Normperiode 1981-2010, Tech. Rep. 245, Fachbericht MeteoSchweiz, 2013.
- Bordoy, R. and Burlando, P.: Stochastic downscaling of precipitation to high-resolution scenarios in orographically complex regions: 1. Model evaluation, *Water Resources Research*, 50, 540–561, 2014.
- 10 Charles, S. P., Bates, B. C., and Hughes, J. P.: A spatiotemporal model for downscaling precipitation occurrence and amounts, *Journal of Geophysical Research: Atmospheres*, 104, 31 657–31 669, 1999.
- Chiew, F., Kirono, D., Kent, D., a.J. Frost, Charles, S., Timbal, B., Nguyen, K., and Fu, G.: Comparison of runoff modelled using rainfall from different downscaling methods for historical and future climates, *Journal of Hydrology*, 387, 10–23, <https://doi.org/10.1016/j.jhydrol.2010.03.025>, 2010.
- 15 Dee, D. P., Uppala, S. M., Simmons, A. J., Berrisford, P., Poli, P., Kobayashi, S., Andrae, U., Balmaseda, M. A., Balsamo, G., Bauer, P., Bechtold, P., Beljaars, A. C. M., van de Berg, L., Bidlot, J., Bormann, N., Delsol, C., Dragani, R., Fuentes, M., Geer, A. J., Haimberger, L., Healy, S. B., Hersbach, H., Hólm, E. V., Isaksen, I., Kållberg, P., Köhler, M., Matricardi, M., McNally, A. P., Monge-Sanz, B. M., Morcrette, J.-J., Park, B.-K., Peubey, C., de Rosnay, P., Tavolato, C., Thépaut, J.-N., and Vitart, F.: The ERA-Interim reanalysis: configuration and performance of the data assimilation system, *Q. J. Roy. Meteor. Soc.*, 137, 553–597, <https://doi.org/10.1002/qj.828>, 2011.
- 20 Deidda, R.: Multifractal analysis and simulation of rainfall fields in space, *Physics and Chemistry of the Earth, Part B: Hydrology, Oceans and Atmosphere*, 24, 73–78, 1999.
- Deidda, R.: Rainfall downscaling in a space-time multifractal framework, *Water Resources Research*, 36, 1779–1794, 2000.
- D’Onofrio, D., Palazzi, E., von Hardenberg, J., Provenzale, A., and Calmanti, S.: Stochastic rainfall downscaling of climate models, *Journal of Hydrometeorology*, 15, 830–843, 2014.
- 25 Ferraris, L., Gabellani, S., Rebora, N., and Provenzale, A.: A comparison of stochastic models for spatial rainfall downscaling, *Water Resour. Res.*, 39, 1368, <https://doi.org/10.1029/2003WR002504>, 2003.
- Harris, D., Menabde, M., Seed, A., and Austin, G.: Multifractal characterization of rain fields with a strong orographic influence, *J. Geophys. Res.*, 101, 26,405–26,414, 1996.
- Haylock, M., Hofstra, N., Klein Tank, A., Klok, E., Jones, P., and New, M.: A European daily high-resolution gridded data set of surface temperature and precipitation for 1950–2006, *Journal of Geophysical Research: Atmospheres*, 113, 2008.
- 30 Hijmans, R. J., Cameron, S. E., Parra, J. L., Jones, P. G., and Jarvis, A.: Very high resolution interpolated climate surfaces for global land areas, *International journal of climatology*, 25, 1965–1978, 2005.
- Hijmans, R. J., Cameron, S. E., Parra, J. L., Jones, P. G., and Jarvis, A.: WorldClim: Global weather stations, <https://databasin.org/datasets/15a31dec689b4c958ee491ff30fce75>, 2010.
- 35 Jothityangkoon, C., Sivapalan, M., and Viney, N. R.: Tests of a space-time model of daily rainfall in southwest Australia based on nonhomogeneous random cascades, *Water Resour. Res.*, 36, 267–284, 2000.



- Kotlarski, S., Keuler, K., Christensen, O. B., Colette, A., Déqué, M., Gobiet, A., Goergen, K., Jacob, D., Lüthi, D., van Meijgaard, E., et al.: Regional climate modeling on European scales: A joint standard evaluation of the EURO-CORDEX RCM ensemble, *Geoscientific Model Development Discussions*, 7, 217–293, 2014.
- Lovejoy, S. and Mandelbrot, B.: Fractal properties of rain and a fractal model, *Tellus*, 37A, 209–232, 1985.
- 5 Lovejoy, S. and Schertzer, D.: Multifractals, cloud radiances and rain, *Journal of Hydrology*, 322, 59–88, 2006.
- Maraun, D., Wetterhall, F., Ireson, A., Chandler, R., Kendon, E., Widmann, M., Brienen, S., Rust, H., Sauter, T., Themeßl, M., and Others: Precipitation downscaling under climate change. Recent developments to bridge the gap between dynamical models and the end user, *Reviews of Geophysics*, pp. 1–38, <https://doi.org/10.1029/2010RG000314>, 2010.
- Mehrotra, R. and Sharma, A.: A nonparametric stochastic downscaling framework for daily rainfall at multiple locations, *Journal of Geophysical Research: Atmospheres*, 111, 2006.
- 10 Palazzi, E., von Hardenberg, J., Terzago, S., and Provenzale, A.: Precipitation in the Karakoram-Himalaya: a CMIP5 view, *Climate Dynamics*, 45, 21–45, 2015.
- Pathirana, A. and Herath, S.: Multifractal modelling and simulation of rain fields exhibiting spatial heterogeneity, *Hydrol. Earth Syst. Sci.*, 6, 659–708, 2002.
- 15 Peterson, A. and Nakazawa, Y.: Environmental data sets matter in ecological niche modelling: an example with *Solenopsis invicta* and *Solenopsis richteri*, *Global ecology and Biogeography*, 17, 135–144, 2008.
- Pieri, A. B., von Hardenberg, J., Parodi, A., and Provenzale, A.: Sensitivity of Precipitation Statistics to Resolution, Microphysics, and Convective Parameterization: A Case Study with the High-Resolution WRF Climate Model over Europe, *Journal of Hydrometeorology*, 16, 1857–1872, 2015.
- 20 Purdy, J. C., Harris, D., Austin, G. L., Seed, A. W., and Gray, W.: A case study of orographic rainfall processes incorporating multiscaling characterization techniques, *J. Geophys. Res.*, 106, 7837–7845, 2001.
- Rasmussen, R., Baker, B., Kochendorfer, J., Meyers, T., Landolt, S., Fischer, A. P., Black, J., Thériault, J. M., Kucera, P., Gochis, D., et al.: How well are we measuring snow: The NOAA/FAA/NCAR winter precipitation test bed, *Bulletin of the American Meteorological Society*, 93, 811–829, 2012.
- 25 Reborá, N., Ferraris, L., von Hardenberg, J., and Provenzale, A.: The RainFARM: Rainfall Downscaling by a Filtered AutoRegressive Model, *J. Hydrometeorol.*, 7, 724–738, 2006.
- Rodriguez-Iturbe, I., Cox, D. R., and Isham, V.: Some Models for Rainfall Based on Stochastic Point Processes, *Proceedings of the Royal Society of London A: Mathematical, Physical and Engineering Sciences*, 410, 269–288, <https://doi.org/10.1098/rspa.1987.0039>, 1987.
- Rodriguez-Iturbe, I., Cox, D., and Isham, V.: A point process model for rainfall: further developments, in: *Proceedings of the Royal Society of London A: Mathematical, Physical and Engineering Sciences*, vol. 417, pp. 283–298, The Royal Society, 1988.
- 30 Roe, G. H.: Orographic precipitation, *Ann. Rev. Earth and Planet. Sci.*, 33, 645–671, <https://doi.org/10.1146/annurev.earth.33092203.122541>, 2005.
- Smith, R. B.: Progress on the theory of orographic precipitation, in: *Tectonics, Climate and Landscape Evolution*, Special paper 398, edited by Willet et al., S. D., chap. 1, pp. 1–16, Geological Society of America, 2006.
- 35 Townsend Peterson, A., Papeş, M., and Eaton, M.: Transferability and model evaluation in ecological niche modeling: a comparison of GARP and Maxent, *Ecography*, 30, 550–560, 2007.
- Turco, M., Zollo, A., Ronchi, C., Luigi, C. D., and Mercogliano, P.: Assessing gridded observations for daily precipitation extremes in the Alps with a focus on northwest Italy, *Natural Hazards and Earth System Sciences*, 13, 1457–1468, 2013.



- Viterbo, F., von Hardenberg, J., Provenzale, A., Molini, L., Parodi, A., Sy, O. O., and Tanelli, S.: High-Resolution Simulations of the 2010 Pakistan Flood Event: Sensitivity to Parameterizations and Initialization Time, *J. Hydrometeorol.*, 17, 1147–1167, <https://doi.org/10.1175/JHM-D-15-0098.1>, 2016.
- von Hardenberg, J., Ferraris, L., and Provenzale, A.: The shape of convective rain cells, *Geophysical research letters*, 30, 2003.
- 5 Vrac, M. and Naveau, P.: Stochastic downscaling of precipitation: From dry events to heavy rainfalls, *Water resources research*, 43, 2007.
- Waltari, E., Hijmans, R. J., Peterson, A. T., Nyári, Á. S., Perkins, S. L., and Guralnick, R. P.: Locating Pleistocene refugia: comparing phylogeographic and ecological niche model predictions, *PLoS one*, 2, e563, 2007.
- Warren, D. L. and Seifert, S. N.: Ecological niche modeling in Maxent: the importance of model complexity and the performance of model selection criteria, *Ecological Applications*, 21, 335–342, 2011.
- 10 Wilks, D.: Multisite generalization of a daily stochastic precipitation generation model, *Journal of Hydrology*, 210, 178–191, 1998.
- Wilks, D. S.: Multisite downscaling of daily precipitation with a stochastic weather generator, *Climate Research*, 11, 125–136, 1999.

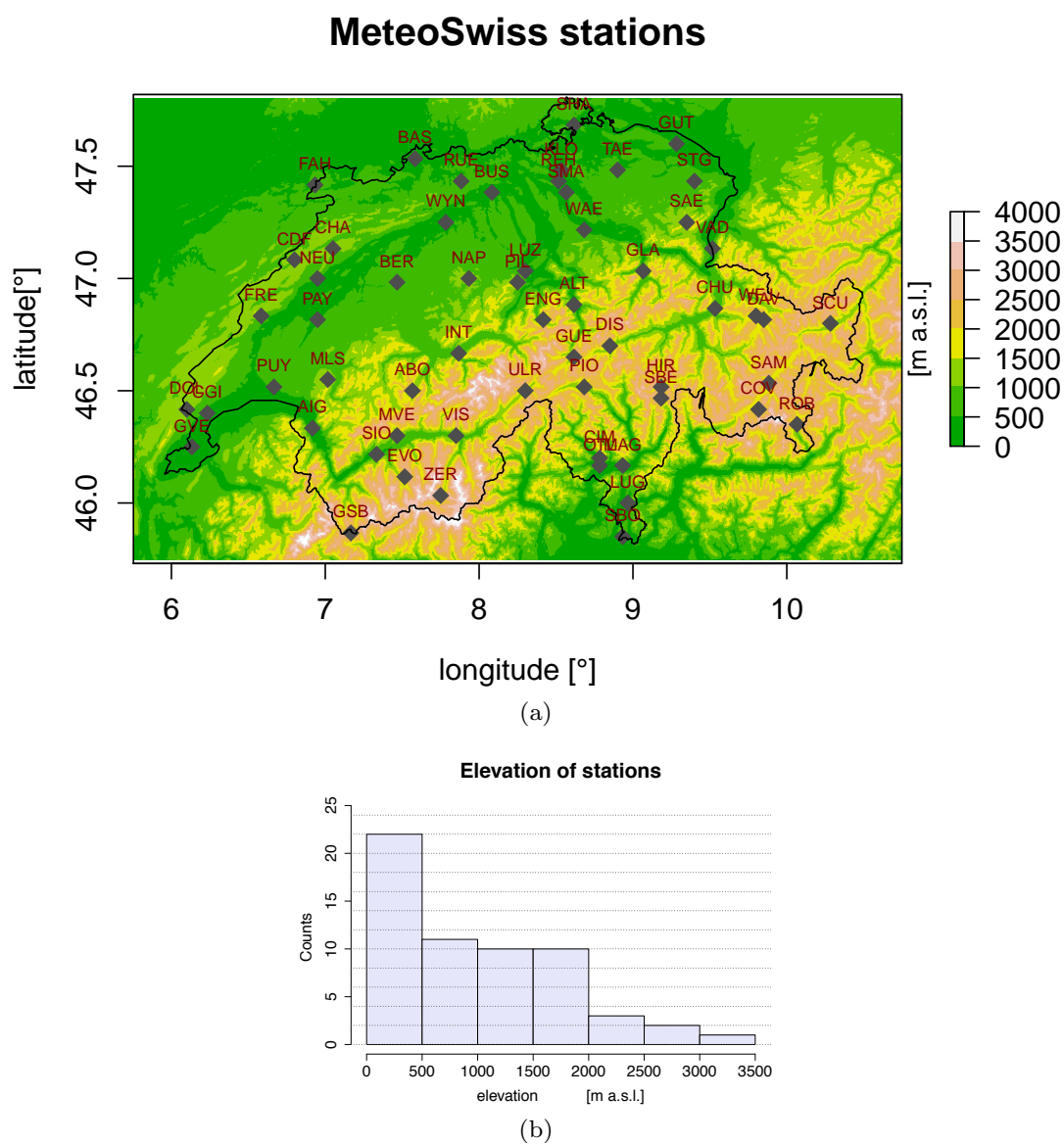


Figure 1. (a) Orography of the study area including the Swiss Alps, according to a 500m resolution digital elevation model. Meteorological stations of the MeteoSwiss network providing at least 80% of valid daily total precipitation data over the period 1981-2010 are labelled with gray diamonds. (b) Distribution of the elevations of the MeteoSwiss stations grouped in 500 m bins.

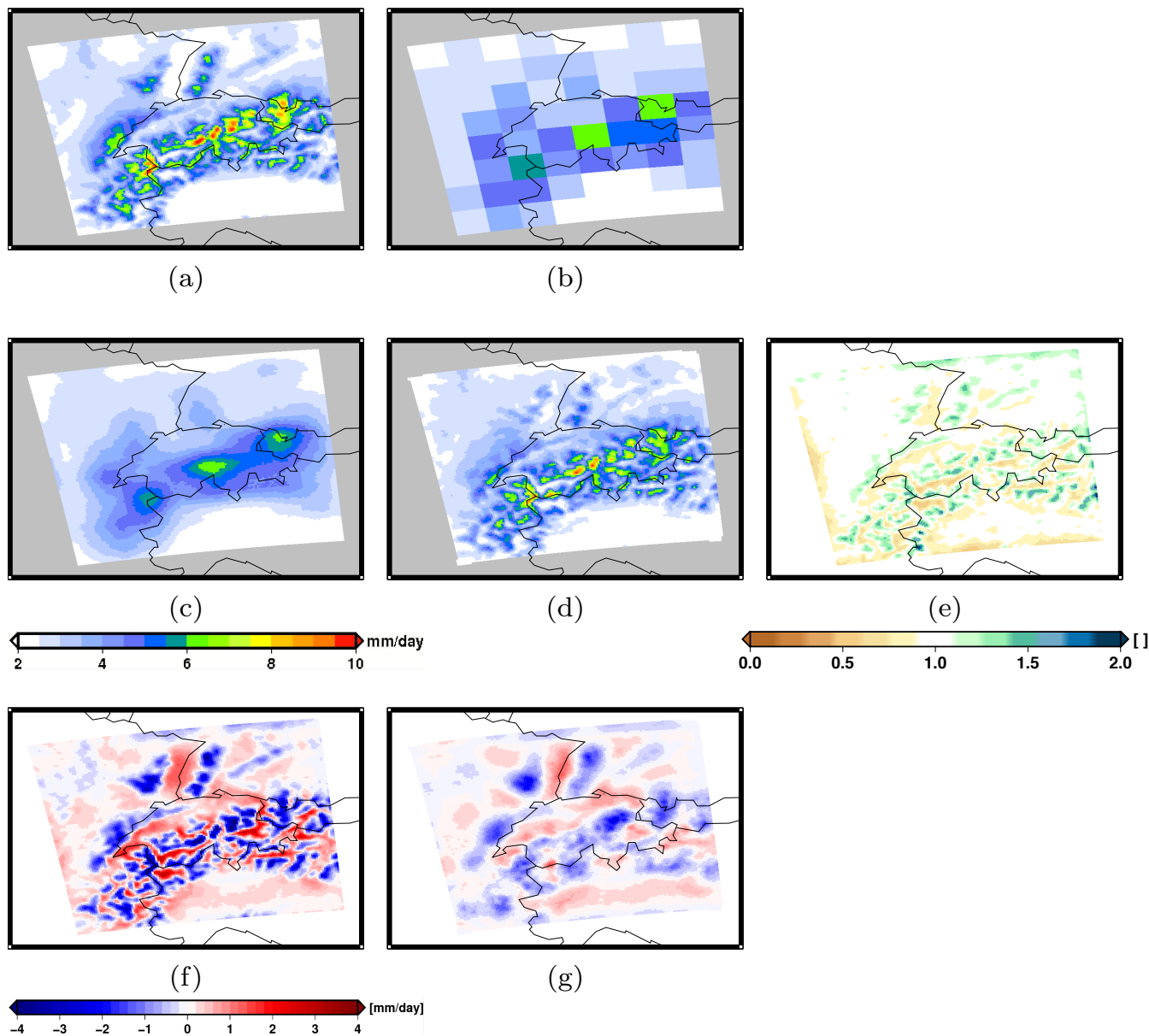


Figure 2. The “perfect model” experiment. Average precipitation climatology (1980-2008) derived from: (a) high-resolution WRF daily fields at 4 km, here considered as the “truth”; (b) WRF daily fields aggregated at 64 km, i.e. the fields, $P(X, Y, t)$, to be downscaled; (c) $P(X, Y, t)$ downscaled at 4 km using the standard RainFARM method; (d) $P(X, Y, t)$ downscaled at 4 km using the modified RainFARM method; (e) example of map of weights obtained in this case for the month of June; (f-g) anomalies of the downscaled climatologies in plots (c) and (d) with respect to the reference precipitation field (a).

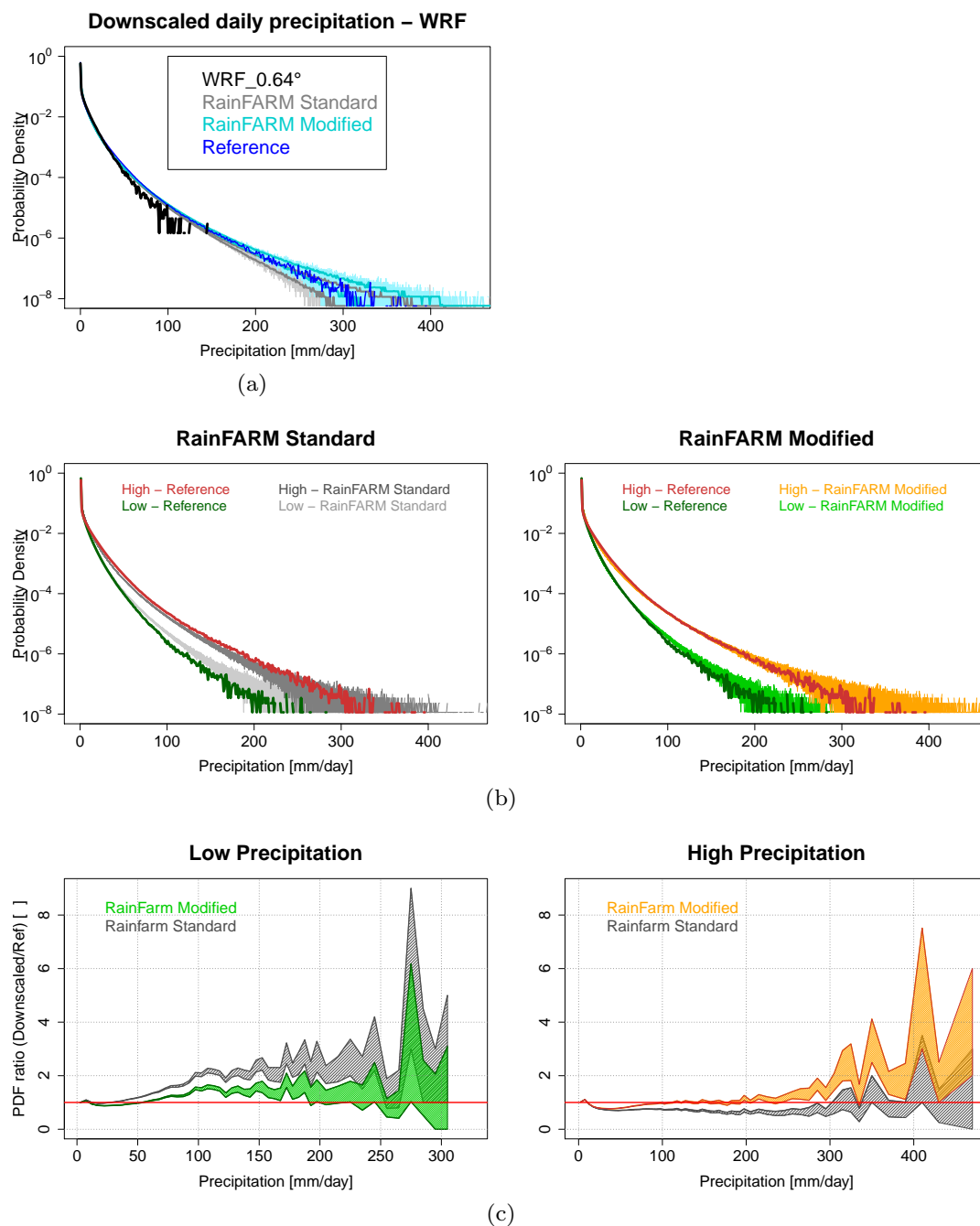


Figure 3. The “perfect model” experiment: (a) Probability density function (PDF) of WRF daily precipitation at coarse resolution (64 km, black), of the downscaled WRF precipitation (from 64 km to 4 km) obtained using the standard (gray) and modified (light blue) RainFARM methods, compared to the original fine-resolution (4 km) WRF precipitation (blue). Gray and light-blue bands and lines represent the spread of the ensemble and the 10–90th percentile range, respectively, calculated from 80 realizations of the stochastic downscaled field; (b) same as (a) but separating high- and low-precipitation grid-points as specified in the text; (c) ratio between the PDF of WRF downscaled precipitation and the PDF of the reference, for low- and high-precipitation grid-points, with the standard and the modified RainFARM methods.

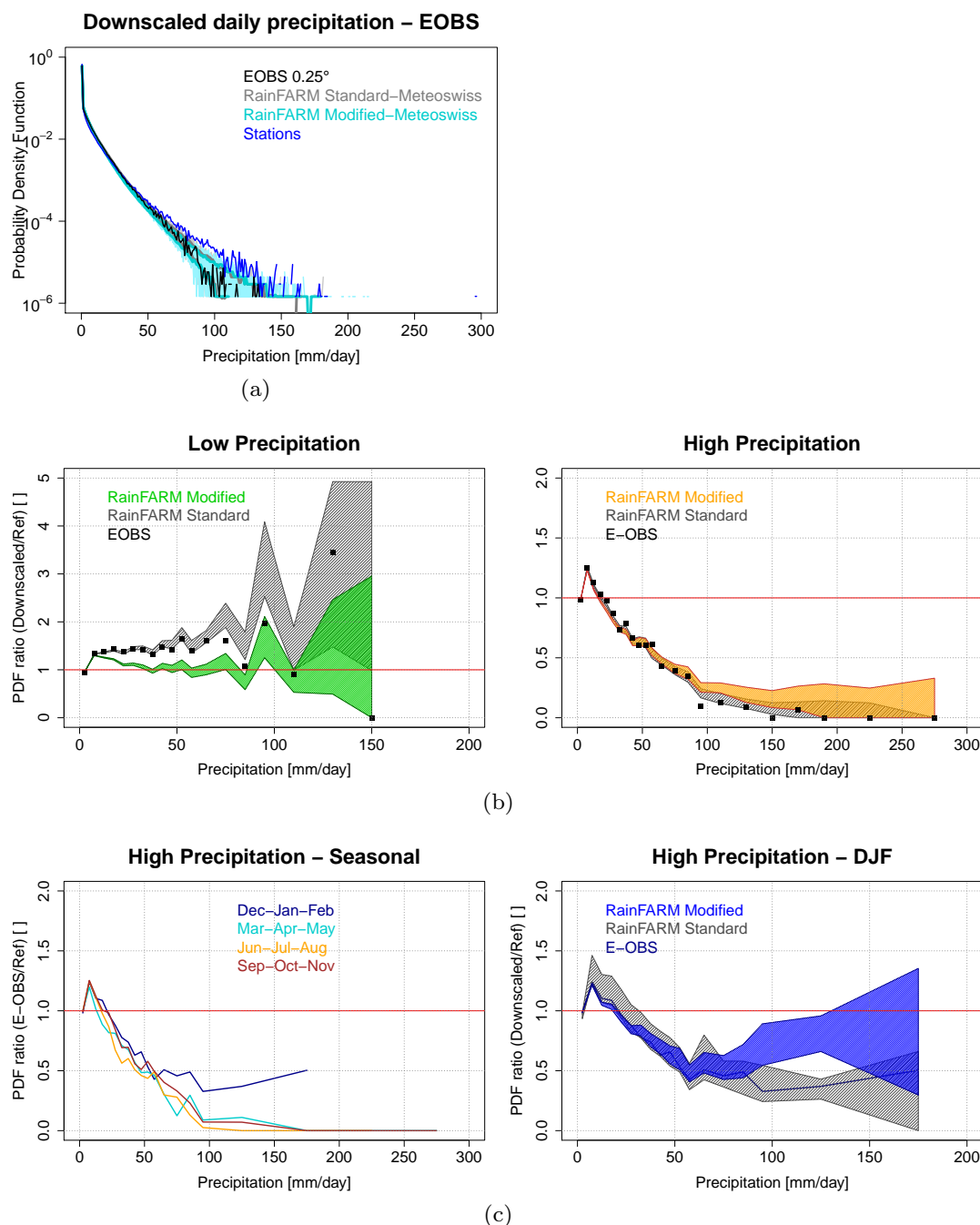


Figure 4. (a) The “real case” experiment. Probability density function (PDF) of: E-OBS daily precipitation at the original resolution of 0.25°; E-OBS precipitation downscaled using the standard (gray) and the modified (light blue) RainFARM with the MeteoSwiss RNormM weights; the observations from 59 rain gauge stations in Switzerland (dark blue). Gray and light-blue bands and lines represent the spread of the ensemble and the 10-90th percentile ranges, respectively, calculated from 80 realizations of the stochastic downscaled field; (b) ratio between the PDF of E-OBS downscaled precipitation and the PDF of the station observations, for low (left) and high (right) precipitation grid-points, comparing the standard and the modified RainFARM methods; (c, left) ratios between the PDF of E-OBS daily precipitation and the PDF of the station observations for different seasons (DJF, MAM, JJA, SON); (c, right) ratios between the PDF of E-OBS downscaled precipitation for DJF, and the PDF of the station observations, for high-precipitation gridpoints.

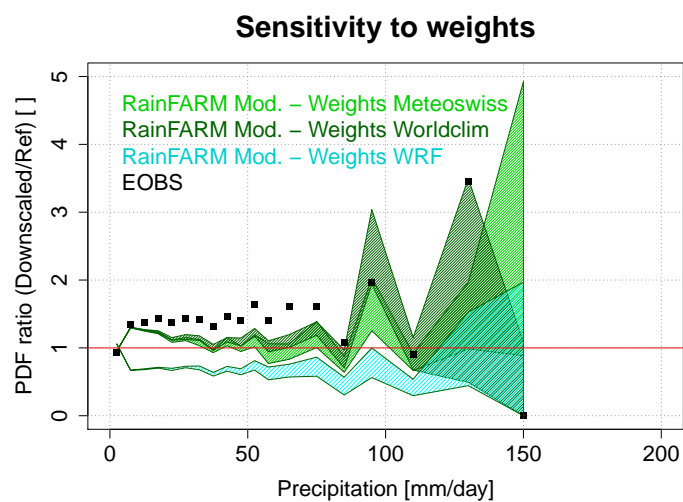


Figure 5. Sensitivity of the modified RainFARM downscaling method to different weights, derived from MeteoSwiss (light green), WorldClim (dark green) and WRF (cyan) climatologies respectively, for low precipitation gridpoints. The bands refers to the 10-90th percentile interval calculated over 10 downscaling realizations.